Nuclear Analysis for the Light Ion Fusion Power Reactor LIBRA-SP

M.E. Sawan

May 1996

UWFDM-1014

FUSION TECHNOLOGY INSTITUTE

UNIVERSITY OF WISCONSIN

MADISON WISCONSIN

Nuclear Analysis for the Light Ion Fusion Power Reactor LIBRA-SP

M.E. Sawan

Fusion Technology Institute
University of Wisconsin
1500 Engineering Drive
Madison, WI 53706

http://fti.neep.wisc.edu

May 1996

UWFDM-1014

NUCLEAR ANALYSIS FOR THE LIGHT ION
FUSION POWER REACTOR LIBRA-SP

Mohamed E. Sawan

Fusion Technology Institute, University of Wisconsin-Madison
1500 Engineering Drive
Madison, WI 53706-1687
(608) 263-5093

ABSTRACT

A 1.2 m thick zone of blanket tubes is needed for the LIBRA-SP chamber wall to be a lifetime component. The roof should be located at 17 m from the target to be a lifetime component. The depth of the LiPb pool should be 0.6 m for the bottom plate to be a lifetime component. The required biological shield thickness is 2.5 m on the side and 2.6 m at the top. The overall TBR is 1.435 and the overall energy multiplication is 1.18. The diode casing as well as the cathode and anode feed bus-bars are lifetime components. If ceramic insulators are used in the magnet coils, they will be lifetime components. If organic insulators are used, the coils have to be replaced once in the life of the reactor.

I. INTRODUCTION

LIBRA-SP is a 1000 MWe light ion beam power reactor design study which utilizes a self-pinched mode for propagating the ions from the ion-diode to the target.[1] The reactor is driven by 7.2 MJ of 30 MeV Li ions at a repetition rate of 3.88 Hz and a target yield of 589 MJ. A schematic picture of the LIBRA-SP target chamber is shown in Fig. 1.

A novel scheme of first wall protection is used. Rigid ferritic steel tubes called PERIT (perforated rigid tubes) units are used. These tubes are equipped with tiny nozzles that spray vertical fans of liquid metal, overlapping each other such that the front two rows of tubes are completely shadowed from the target emanations. Behind the blanket is a 50 cm thick HT-9 reflector which is also the vacuum boundary. The whole chamber is surrounded by a steel reinforced concrete shield.

In this paper, the results of the neutronics analysis performed for LIBRA-SP are presented. The dimensions of the different reactor regions are determined for the design goals to be achieved. In addition, the lifetimes for the PERIT tubes and diode components are identified.

II. CHAMBER NEUTRONICS ANALYSIS

Neutronics analysis has been performed for the chamber using one-dimensional spherical geometry calculations for the regions surrounding the target. The discrete ordinates code ONEDANT[2] was utilized along with cross section data based on the most recent ENDF/B-VI nuclear data evaluation.[3] A point source is used at the center of the chamber emitting neutrons and gamma photons with the LIBRA-SP target spectrum. The results are normalized to the fusion power of 2285 MW.

A. PERIT Tube Region

The neutronics analysis aimed at determining the blanket design that satisfies tritium self-sufficiency, large energy multiplication (M), and wall protection requirements. The blanket is made of banks of PERIT tubes with 0.5 packing fraction. The $Li_{17}Pb_{83}$ eutectic with 90% ^6Li enrichment is the breeder and coolant. The tubes are made of the ferritic steel alloy HT-9 and consist of 8 vol.% HT-9 and 92 vol.% $Li_{17}Pb_{83}$. A 0.5 m thick reflector consisting of 90 vol.% HT-9 and 10 vol.% $Li_{17}Pb_{83}$ is used behind the blanket. A minimum local (1-D) tritium breeding ratio (TBR) of 1.3 is required in the PERIT tubes and reflector to achieve overall tritium self-sufficiency without a breeding blanket in the roof. In addition, the PERIT tubes are required to provide adequate
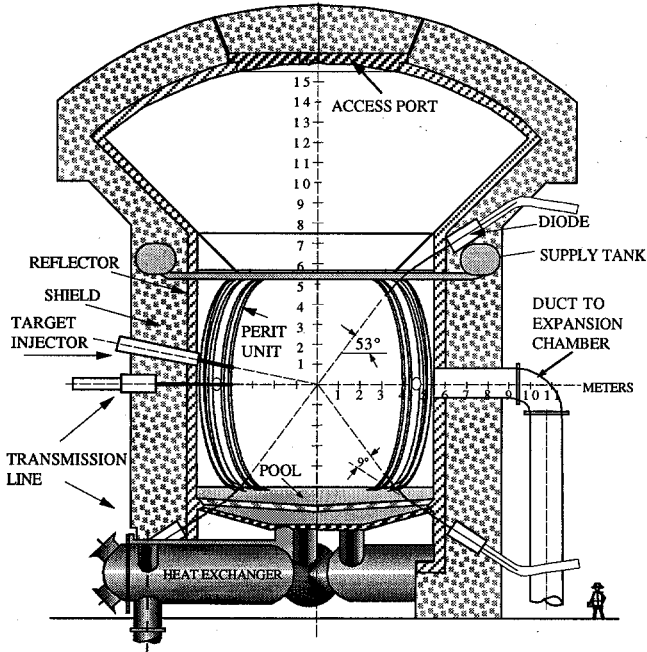
Fig. 1. Cross-sectional view of the reactor chamber.

protection for the front of the reflector (chamber wall) to make it last for the whole reactor life. We adopted a conservative end-of-life dpa limit of 150 dpa for HT-9.

The required thickness of the PERIT tube zone (blanket) was determined to be 1.2 m. The inner chamber wall radius is 5.2 m implying that the front surface of the PERIT units is at a radius of 4 m and is exposed to a neutron wall loading of 7.4 MW/m^2. The peak dpa rate in the PERIT units is 94.2 dpa/FPY implying a lifetime of 1.6 FPY. A gradual reduction in the damage rate is obtained as one moves toward the back of the blanket. The peak helium production rate is 436 He appm/FPY. The peak dpa rate in the chamber wall is 4.2 dpa/FPY implying an end-of-life damage of only 126 dpa. The peak helium production rate is only 0.9 He appm/FPY.

The local TBR is 1.481 and the local blanket and reflector nuclear energy multiplication M_n, defined as the ratio of nuclear heating to the energy of incident neutrons and gamma photons, is 1.285. The power density peaks at 18.3 W/cm^3 in the front PERIT tubes and drops to 2.4 W/cm^3 in the back tubes. The peak power density in the chamber wall is 0.52 W/cm^3.

B. Reactor Roof

The roof of the chamber is a large dome that is required to be a lifetime component. The roof is 50 cm thick and consists of 90 vol.% HT-9 and 10 vol.% Li$_{17}$Pb$_{83}$. The roof of the LIBRA-SP chamber is located at 17 m from the target to ensure that it lasts for the whole reactor life. The roof is exposed to a neutron wall loading of 0.41 W/cm^2. The peak dpa and helium production rates in the HT-9 roof are 4.88 dpa/FPY and 23.6 He appm/FPY, respectively. The end-of-life (30 FPY) peak damage in the roof is 146 dpa implying that it is a lifetime component. The local TBR and M_n values are 0.499 and 1.349, respectively.

C. Bottom Pool

The bottom of the chamber consists of a lithium lead pool which is formed by the coolant flowing through the PERIT tubes. It drains through a 25 cm thick perforated plate made of HT-9, which acts as a shock damper. This perforated splash plate consists of 80 vol.% HT-9 and 20 vol.% Li$_{17}$Pb$_{83}$. The LiPb drains into a sump leading to an intermediate heat exchanger. The LiPb thickness in the sump is taken to be 0.3 m. The depth of the LiPb pool at the bottom of the reactor was determined to be 0.6 m to allow the bottom perforated plate to be a lifetime component. The surface of the pool at 5 m from the target is exposed to a neutron wall loading of 4.74 W/cm^2. The peak dpa and helium production rates in the plate are 4 dpa/FPY and 1.04 He appm/FPY, respectively. The end-of-life peak damage in the plate is only 120 dpa implying that it will be a lifetime component. The local TBR and M_n values are 1.592 and 1.273, respectively.

D. Biological Shield Design

The reactor shield is designed such that the occupational biological dose rate outside the shield does not exceed 2.5 mrem/hr during reactor operation. The biological shield consists of 70 vol.% concrete, 20 vol.% carbon steel C1020 and 10 vol.% He coolant. The required biological shield thickness was determined for both the reactor side and reactor roof. Fig. 2 gives the dose rate at the back of the shield at the reactor midplane as a function of shield thickness. A 2.5 m thick shield is required to yield an acceptable operational dose rate of 2.23 mrem/hr. The results for the roof indicate that the biological shield thickness above the roof should be 2.6 m thick. This yields an acceptable operational dose rate of 1.8 mrem/hr.
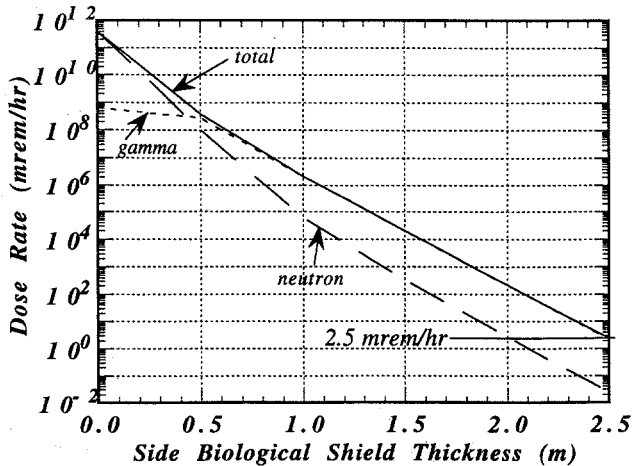
Fig. 2. Effect of side biological shield thickness on dose rate during reactor operation.

E. Overall Reactor Chamber Neutronics Parameters

Using the coverage fractions and local nuclear parameters calculated for the different reactor regions, the overall reactor TBR and M_n can be determined. There are 24 beam ports with a diameter of 2 cm each. Only 0.004% of the source neutrons stream directly into these ports. Source neutrons in a cone with conical angle of 26.56° will impinge directly on the roof. Similarly, source neutrons directed towards the pool in a cone with the same conical angle will impinge directly on the pool. The rest of the source neutrons will go directly to the PERIT tubes in the reactor side. The results indicate that the overall TBR and M_n values in LIBRA-SP are 1.435 and 1.288, respectively. To take into account the surface energy deposited by x-rays and ion debris and the energy lost in target endoergic reactions, an overall energy multiplication factor (M_o) is defined as the ratio of total power deposited to the DT fusion power. For the target design used here, the overall energy multiplication for the reference LIBRA-SP design is 1.18 implying a total power of 2695 MW deposited in the chamber with 784 MW deposited at the front surfaces by x-rays and debris and 1911 MW deposited volumetrically by neutrons and gamma photons.

III. NEUTRONICS ANALYSIS FOR THE DIODES

A. Calculational Method

Radiation damage to the sensitive components of the diodes is affected by the detailed geometrical configuration and neutron streaming through the ports. A multidimensional neutronics calculation is required to properly model the complicated geometrical configuration. Two-dimensional neutronics calculations have been performed to estimate the expected damage levels in the diode components. The discrete ordinates code TWODANT[4] was utilized along with the ENDF/B-VI cross section data.

The region around a beam penetration was modeled in r-z geometry with the target represented by an isotropic point source on the z-axis. This included, in addition to the diode itself, the PERIT region, the reflector, the biological shield and the rotating discs. The two-dimensional model used in the calculations is shown in Fig. 3. A right-reflecting boundary is used at a radius of 1.5 m which is roughly half the distance between the centerlines of adjacent diodes. The calculation utilizes a total of 9196 mesh points. An inherent problem associated with multidimensional discrete ordinates calculations with localized sources is referred to as the "ray effect." It is related to the inability to exactly represent the angular flux component in the normal direction ($\mu = 1$) along the beam penetration. The ray effect has been fully mitigated by use of the first collision method.[5]

B. Radiation Damage Considerations

The diode components most sensitive to radiation damage are the diode casing, cathodes, anodes, and the magnets. The diode casing as well as the cathodes and anodes are assumed to be made of type 304 stainless steel. A conservative end-of-life dpa limit of 150 dpa is assumed. In the magnet coils, we are concerned with both electrical and mechanical degradation from neutron-induced transmutations. An additional irradiation problem is radiolytic decomposition of the water coolant, leading to corrosion and erosion product formation. Among these mechanisms the neutron-induced swelling in the ceramic insulator was found during the MARS[6] study as lifetime limiting for the normal magnet. Spinel ($MgO \cdot Al_2O_3$) is of particular interest in the high-neutron-irradiation environment. Assuming that a 3 vol.% neutron induced swelling in polycrystalline spinel can be accommodated without causing stress problems, the neutron-fluence limit for spinel is 4×10^{22} n/cm^2 ($E > 0.1$ MeV) in the temperature range 100 to 300°C. If an organic insulator such as epoxy or polyimide is used in the magnet, the dose limit will be more restrictive. Based on existing experimental data, the total absorbed dose in the insulator should not exceed $\sim 5 \times 10^9$ Rads[7] to avoid significant degradation in mechanical strength. This corresponds to a fast neutron fluence of $\sim 5 \times 10^{18}$ n/cm^2 ($E > 0.1$ MeV)
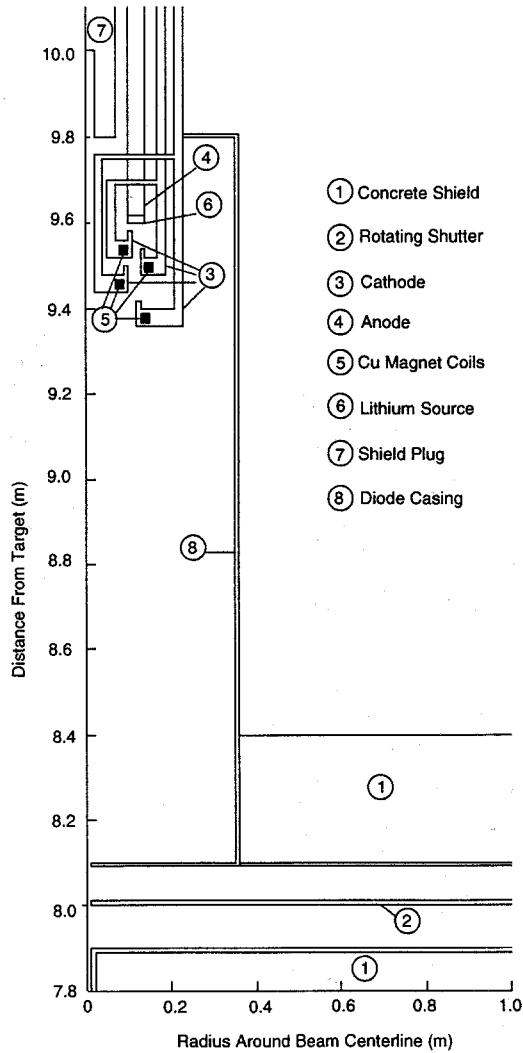
Fig. 3. The r-z two-dimensional neutronics model.

which is about four orders of magnitude lower than the limit for ceramic insulators.

C. Proposed Design Modifications

Since the beam port diameter is only 2 cm, no source neutrons will impinge directly on the anode, cathodes, magnets and diode casing. To reduce the flux and consequently the damage in the diode components, a neutron trap is utilized in the shield plug. Such a trap reduces the neutron flux in the diode components by about an order of magnitude. Additional reduction can be achieved by tapering the inner surface of the beam tube along the direct line-of-sight of source neutrons. This ensures that no source neutrons will impinge directly on the beam tubes and produce secondary neutrons that will stream into the diode. Using this simple geometrical modification in the diode, components will be exposed only to sec-

ondary neutrons produced in the neutron trap. These secondary neutrons can be reduced more by locating the neutron trap farther away from the target. The model used here assumes that the neutron trap is located at 10 m from the target. In addition, the beam tube is not tapered because of the limitations on modeling the geometry for two-dimensional calculations. Hence, the results presented here are conservative and lower flux and damage levels will result from three-dimensional calculations with the geometrical modifications, discussed above, properly modeled.

D. Radiation Damage in Diode Components

The damage in the diode casing peaks at locations adjacent to the cathodes. This is due to the contribution from secondary neutrons produced in the diode components. The peak dpa and helium production rates in the diode casing are 1.9×10^{-4} dpa/FPY and 6.8×10^{-4} He appm/FPY, respectively. The end-of-life peak dpa and helium production in the coil casing are 0.006 dpa and 0.02 He appm, respectively. These very low damage levels imply that the diode casing is a lifetime component.

Damage in the cathode feeds peaks at 10 m from the target where the neutron trap is located. The peak dpa rates are 1.38×10^{-3} and 8×10^{-4} dpa/FPY for the inner and outer cathode feeds, respectively. This leads to peak end-of-life damage levels of only 0.041 and 0.024 dpa implying that the cathode feeds will be lifetime components. Damage in the anode feed, which is closer to the neutron trap, is higher than that in the cathode feeds and the casing. The peak damage rate is 5.5×10^{-3} dpa/FPY and the end-of-life damage is 0.165 dpa. This is still about three orders of magnitude lower than the damage limit.

Table I gives the peak end-of-life dpa and helium production at the tips of the four cathode components. These are identified as cathode A, B, C, and D in the order of distance from the target with cathode A being the farthest. These damage levels are lower than those in the cathode feeds. The end-of-life damage levels at the cathode tips are very small with the largest being only 0.006 dpa for the cathode tip closest to the neutron trap (cathode A).

The end-of-life fast neutron fluence ($E > 0.1$ MeV) is given in Table II for the four magnet coils located in the cathode components. The neutron fluence values are comparable for the four coils with the largest fluence being 8.67×10^{18} n/cm^2 for cathode D. These values are much lower than the 4×10^{22} n/cm^2 fluence limit for ceramic insulators. Hence, if ceramic

TABLE I

Damage in the Cathode Tips After 30 FPY

	dpa	He appm
Cathode A	6.12×10^{-3}	1.03×10^{-2}
Cathode B	4.00×10^{-3}	3.48×10^{-3}
Cathode C	3.51×10^{-3}	3.42×10^{-3}
Cathode D	4.29×10^{-3}	6.78×10^{-3}

TABLE II

End-of-Life Fast Neutron Fluence
in the Magnet Coils

	Fast Neutron Fluence $(E > 0.1$ MeV$)$
Cathode A	7.65×10^{18}
Cathode B	6.39×10^{18}
Cathode C	6.12×10^{18}
Cathode D	8.67×10^{18}

insulators are used in the coils, they will be lifetime components. On the other hand, coils utilizing organic insulators might need to be replaced once during the reactor life. However, it should be noted that coil replacement might not be needed even with organic insulation if the geometrical modifications proposed are implemented. This needs to be confirmed by three-dimensional calculations. The peak end-of-life dpa and helium production in the neutron trap located at 10 m from the target are 153 dpa and 1914 He appm and the peak nuclear heating is ~ 5 W/cm^3. The higher damage level should not be a concern since the neutron trap is not subject to significant stresses. In addition, moving the trap farther from the target will reduce the damage level.

IV. SUMMARY AND CONCLUSIONS

Neutronics analysis has been performed for the LIBRA-SP chamber. The results indicate that a 1.2 m thick PERIT tube zone is needed for the chamber wall at 5.2 m radius to be a lifetime component. The lifetime of the front row of the PERIT tubes is 1.6 FPY. The roof of the chamber dome, made of HT-9, should be located at 17 m from the target to be a lifetime component. The depth of the LiPb pool was determined to be 0.6 m for the bottom plate to be a lifetime component. The required biological shield thickness is 2.5 m on the side and 2.6 m at the top. Using the coverage fractions and local nuclear parameters calculated for the reactor regions, the overall TBR breeding ratio and energy multiplication are 1.435, and 1.18, respectively. A total power

of 2695 MW is deposited in the chamber with 784 MW of it deposited at the front surfaces by x-rays and ion debris.

Two-dimensional neutronics calculations have been performed to estimate the expected damage levels in the diode components. The diode casing as well as the cathode and anode feed bus-bars are lifetime components. The lifetime of the magnet coils in the cathode depends on the type of insulator used. If ceramic insulators are used, the coils too will be lifetime components. If, however, organic insulators are used, the coils have to be replaced once in the reactor life.

REFERENCES

1. B. Badger, et al., "LIBRA-SP - A Light Ion Fusion Power Reactor Design Study Utilizing a Self-Pinched Mode of Ion Propagation," University of Wisconsin Fusion Technology Institute Report UWFDM-982, June 1995.

2. R. O'Dell, et al., "User's Manual for ONEDANT: A Code Package for One-Dimensional, Diffusion-Accelerated, Neutral Particle Transport," Los Alamos National Laboratory, LA-9184-M, 1989.

3. P. F. Rose, "ENDF/B-VI, The U.S. Evaluated Nuclear Data Library for Neutron Reaction Data," Summary Documentation Report ENDF 201, U.S. National Nuclear Data Center, 1992.

4. R. Alcouffe, et al., "User's Guide for TWO-DANT: A Code Package for Two-Dimensional, Diffusion-Accelerated, Neutral Particle Transport," LA-10049-M, Los Alamos National Laboratory (March 1982).

5. R. Alcouffe, R. O'Dell, and F. Brinkley, Jr., "A First-Collision Source Method that Satisfies Discrete S$_n$ Transport Balance," *Nuclear Eng. & Design*, **105**, 198 (1990).

6. B. G. Logan, et al., "MARS Mirror Advanced Reactor Study Commercial Fusion Electric Plant," Lawrence Livermore National Laboratory, UCRL-53480 (1984).

7. W. Daenner, L. El-Guebaly, M. Sawan, et al., "Neutron Shielding and Its Impact on the ITER Machine Design," *Nucl. Engr. and Design* **16**, 183 (1991).